JOURNAL OF PETROLOGY

Journal of Petrology, 2019, Vol. 60, No. 3, 661–671
doi: 10.1093/petrology/egy117
Advance Access Publication Date: 31 December 2018
Comment and Reply

OXFORD

A Reply to the Comment by Gernon *et al.* on the 'Petrography of the Snap Lake Kimberlite Dyke (Northwest Territories, Canada) and its Interaction with Country Rock Granitoids' by Fulop *et al.* (2018)

Alexandrina Fulop[1]*, Maya Kopylova[2], Stephan Kurszlaukis[3], Luke Hilchie[2,4] and Pamela Ellemers[3]

[1]De Beers—Exploration Canada, 300–515 Consumers Road, Toronto, ON M2J 4Z2, Canada; [2]Department of Earth, Atmospheric and Ocean Sciences, University of British Columbia, 2207 Main Mall, Vancouver, BC V6T 1Z4, Canada; [3]De Beers Canada—Mining, 300–1601 Airport Road NE, Calgary, AB T2E 6Z8, Canada; [4]Department of Earth Sciences, Dalhousie University, 1459 Oxford Street, Halifax, NS B3H 4R2, Canada

*Corresponding author. E-mail: alexandrina.fulop@debeersgroup.com

Received December 6, 2018; Accepted December 9, 2018

Key words: kimberlite; alteration; magma batch; diamond; Snap Lake

The Snap Lake kimberlite dyke (Northwest Territories, Canada) is at the center of controversy, being interpreted as either (1) a rock variously affected by granitoid contamination and related metasomatism of a single batch of kimberlite magma (Fulop *et al.*, 2018) or (2) intrusions of two magma batches (Field *et al.*, 2009; Gernon *et al.*, 2012). This seemingly minor issue of rock interpretation is not accidentally on the forefront of kimberlite petrology; emplacement of several magma batches may cause variations in the diamond grade, and thus may influence the resource model and, ultimately, the economics of diamond mines. The petrological interpretation also gives important insights into the emplacement behaviour of kimberlite magmas. Our Reply to the critique by Gernon *et al.* (2019) of our work (Fulop *et al.*, 2018) discusses the methodological roots of the contrasting opinions on Snap Lake and suggests ways for collection of sound and representative data on kimberlites.

SNAP LAKE ROCK TYPES

The model portraying the Snap Lake dyke as forming by intrusions of two magma batches has been advanced in an earlier publication of Field *et al.* (2009) and a later paper by Gernon *et al.* (2012). Field *et al.* (2009) examined 15 thin sections (table 1 of Field *et al.*, 2009). Fourteen of them were taken in a tightly localized area, within 400 m of each other, whereas the dyke was mined over 5 km along dip. The same thin sections were used for scanning electron microscopy (SEM) and for electron probe microanalysis (EPMA) of mineral chemistry. The rest of the dyke was characterized from digital images scanned using a DMT Core scanner for a single drill core located at the NE extremity of the Snap Lake property and from photographs of underground exposures (figs 2 and 3 of Field *et al.*, 2009). As result of this work, Field *et al.* (2009) divided the Snap Lake kimberlite into Olivine-Rich Kimberlite (ORK) and Olivine-Poor Kimberlite (OPK). The former reportedly has 20–50% olivine and abundant (up to 30%), coarse-grained phlogopite phenocrysts, whereas the latter reportedly contains $<$15% of olivine and only minor, fine-grained phlogopite (Field *et al.*, 2009).

Gernon *et al.* (2012) further mapped the sizes and orientation of olivine macrocrysts in the Snap Lake kimberlite underground in two 'zones' of the dyke, Zone 1 stretching $\sim$600 m along the ramp and Zone 2 comprising several test panels within a 60 m $\times$ 80 m area. They recognized 'at least four magmatic lithofacies', including 'olivine-poor and phlogopite-rich units; an olivine-rich and phlogopite-poor unit, and an olivine- and phlogopite-rich unit' (fig. S1 and supplementary material of Gernon *et al.*, 2012).

Fulop *et al.* (2018) documented the petrography of the Snap Lake kimberlite, its country rocks and xenoliths based on 100 drill cores (a cumulative length of

~1000 m), 30 mapped underground faces (a cumulative surface area of ~300 m^2), 400 thin sections, and 370 whole-rock major and trace element analyses. The sampling locations (figs 1–3 of Fulop *et al.*, 2018) were chosen to ensure a good lateral coverage of the dyke at different thicknesses, in all alteration zones, and all country-rock lithologies. Fulop *et al.* described lithological and mineralogical zonation of the dyke from the relatively fresh HK1 to the highly altered HK6 in contact with wall-rock granitoid. Such zonation was not found in contact with the host metavolcanic rocks. The dyke was interpreted as formed by emplacement of a single batch of magma that experienced post-emplacement alteration. The texture of phlogopite is a discriminant in the Snap Lake kimberlite classification (HK1–HK6) of Fulop *et al.* (2018).

We submit that the mineralogical complexity of the kimberlite and the geological basis for the textural changes were missed by Field *et al.* (2009) and Gernon *et al.* (2012) as a result of their chosen research methodology, leading to erroneous conclusions on the origin of the Snap Lake kimberlite. The following problems illustrate our point.

1. Emphasis of sharp transitions from OPK to ORK. These features, illustrated by underground photographs of Field *et al.* (2009) and Gernon *et al.* (2012, 2019), were oddities and were not found consistently in 4 years of geological observations by De Beers' geologists. Instead, De Beers' mining geologists saw a common uneven distribution of olivine enhanced by alteration (Fig. 1a). Field *et al.* (2009) and Gernon *et al.* (2012) observed similar olivine distributions, but interpreted them as 'autholiths of ORK in OPK'. However, the transitions from 'ORK' to 'OPK' are more commonly gradual, as illustrated in Fig. 2a and b.
2. The lack of recognition of post-emplacement alteration of the kimberlite beyond olivine serpentinization. Field *et al.* (2009) did not discuss alteration of the Snap Lake dyke, and 'profound alteration' of the Snap Lake kimberlite for Gernon *et al.* (2019) meant only the lack of fresh olivine. Other effects of post-emplacement alteration on the mineralogy, texture, and bulk composition were either not recognized, or assigned entirely to magmatic processes. Figure 1 of Gernon *et al.* (2019), which is supposed to cover all the macroscopic features of the Snap Lake kimberlite, does not show a highly altered rock in any of the photographs. In fact, all photographs represent ORK, the least altered rock type. Figure 2a of Gernon *et al.* (2019) presents the only highly altered rock, which also happens to be the only sample corresponding to the definition of OPK of Field *et al.* (2009) and Gernon *et al.* (2012). Yet its mineralogy (beyond olivine serpentinization) is exclusively assigned to magmatic processes (Gernon *et al.*, 2019) without consideration of alteration. This approach clearly contradicts the principle declared by Gernon *et al.* in their Comment that 'textures and features in highly altered rock are the consequence of alteration unless proven otherwise'.
3. Confusion of the appearance of altered kimberlite with OPK. For example, domains of more intensely altered, talc-dominated HK6 in HK1–2 (Fig. 1b) can be mistaken for OPK in the absence of sufficient thin-section observations to confirm the presence of olivine. A relatively sharp transition in the colour of secondary sheet silicates pseudomorphing olivine (Fig. 2b and c), enhanced by the presence of dolomite veins (Fig. 2b), can be misleading in photographs taken underground and in the underground mapping, and confused with a lower mode of olivine.
4. Missing both the link between the secondary alteration and granitoids, and the contrast between the kimberlite–granitoid and the kimberlite–metavolcanic contacts. Figure 3 of Gernon *et al.* (2012) indicates the absence of altered kimberlite lacking visible olivine (called OPK by Field *et al.*, 2009; Gernon *et al.*, 2012) at the margins of the dyke in channel sample 5, where kimberlite is in contact with metavolcanic country rocks, and the presence of 50–120 cm thick OPK in dyke selvages where kimberlite is in contact with granite. Yet Gernon *et al.* (2019) maintain that their work 'found phlogopite-rich margins in the area with metavolcanic country rock'. The consistent adjacency of ORK with metavolcanic contacts and OPK with granite contacts is impossible to explain if ORK and OPK are separate magma batches. Moreover, Field *et al.* (2009) and Gernon *et al.* (2012) did not recognize that kimberlite slabs commonly show 'OPK' as a halo around granite xenoliths (Fig. 1b).
5. The weakness and inconsistency of the criteria established by Field *et al.* (2009) for the OPK–ORK division. The macroscopically estimated olivine abundance in conjunction with the phlogopite abundance estimated in thin sections cannot stand as sound criteria for different rock types that correspond to different magma batches. This can be illustrated by several examples. The first is the existence of the third unit of 'olivine- and phlogopite-rich kimberlite' (supplementary material, fig. S1 of Gernon *et al.*, 2012), which was discussed as a 'textural variant of OPK'. The classification of this phlogopite-rich ORK with OPK asserts the higher significance of the phlogopite mode over the olivine abundance criteria of Field *et al.* (2009) and Gernon *et al.* (2012). Another example of this inconsistency is fig. 3c of Gernon *et al.* (2019), classified by the authors as OPK. The high phlogopite abundance in this sample, typical for OPK, contrasts with the pronounced poikilitic texture of the phlogopite, which is characteristic of ORK (Field *et al.*, 2009). Another instance of misclassified samples is OPK in figs 1c and d of Gernon *et al.* (2019). The samples should be classified as ORK on the basis of the abundant

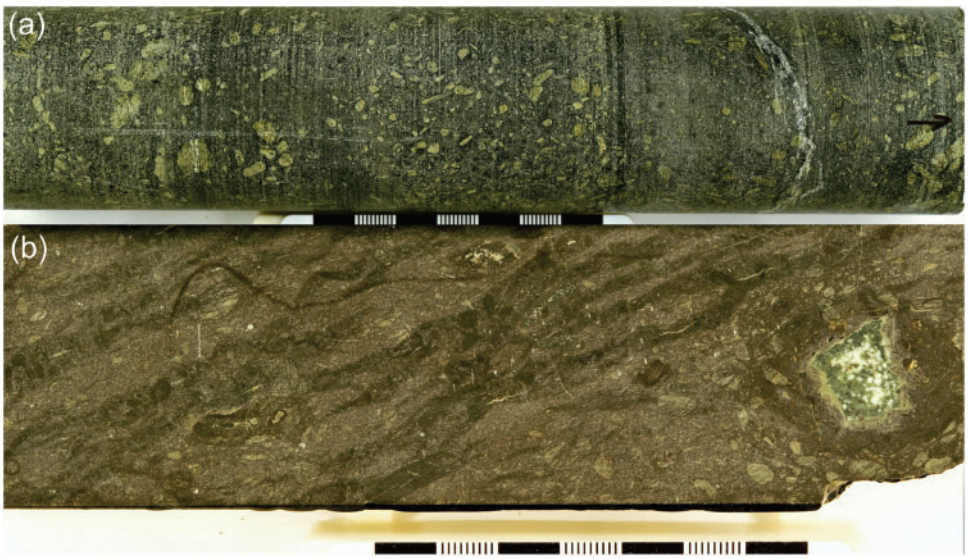

Fig. 1. (a) Uneven distribution of olivine in HK1–2 of core sample 0294. (b) Spatial relationships between variably altered Snap Lake kimberlite in sample 0317. The disappearance of olivine around granite clasts in a halo of a darker green kimberlite (HK5–6) should be noted. Also noteworthy are multiple bands of the similarly dark green kimberlite with no visible olivine that occur in the slab as areas of alteration with a random distribution.

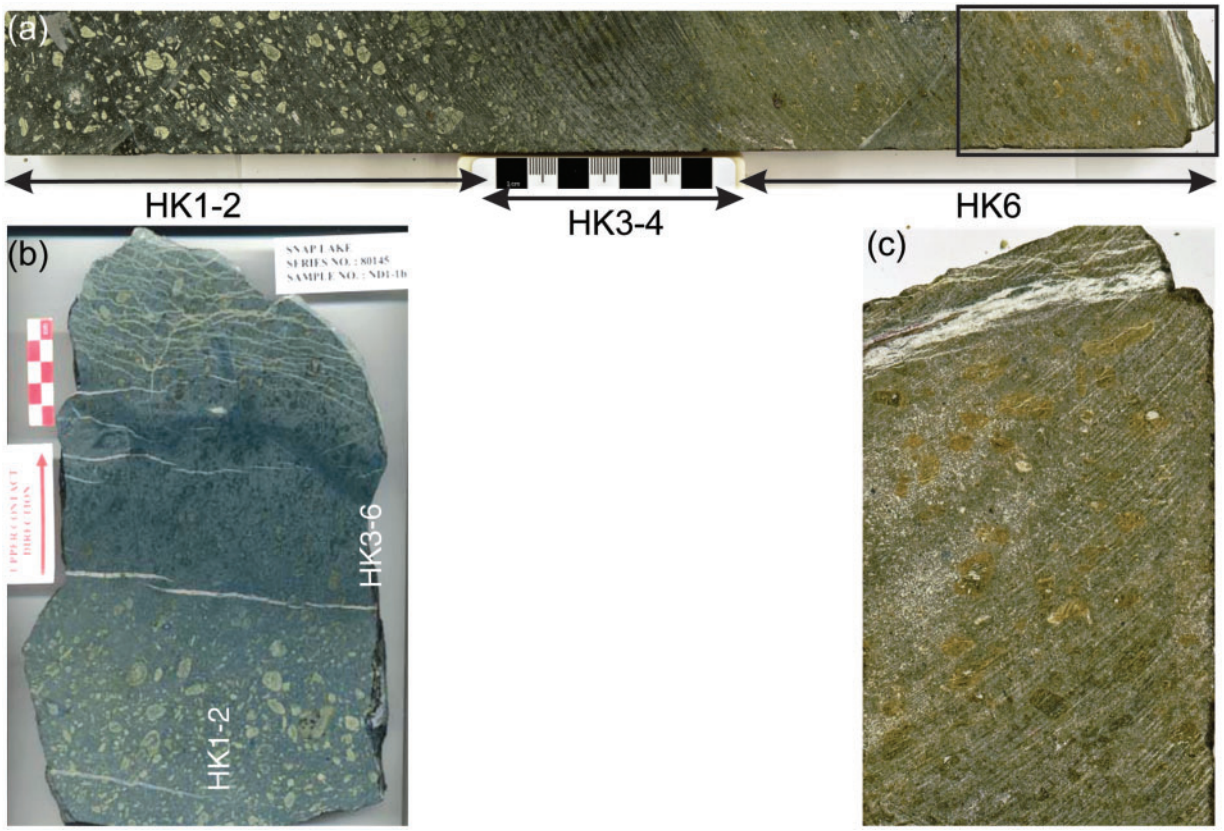

Fig. 2. (a) Core slab 0311 showing a typical zoning from the contact to the center of the dyke. In HK3–4, olivines are visible as dark pseudomorphs; in HK5–6 olivines are either invisible or visible as yellow pseudomorphs. Note the change of the kimberlite groundmass colour from dark green in HK3–4 to lighter yellow–green in HK6 corresponding to the different groundmass mineralogy. (b) Sample ND1-1b showing a sharp transition in the colour of secondary sheet silicates pseudomorphing olivine: dark green in HK6 and yellow–grey in HK1–2. (c) An enlarged rectangle of (a) demonstrates yellow and green patches that used to be olivine macrocrysts. Without the enlargement, or thin sections, the kimberlite may look olivine-poor.

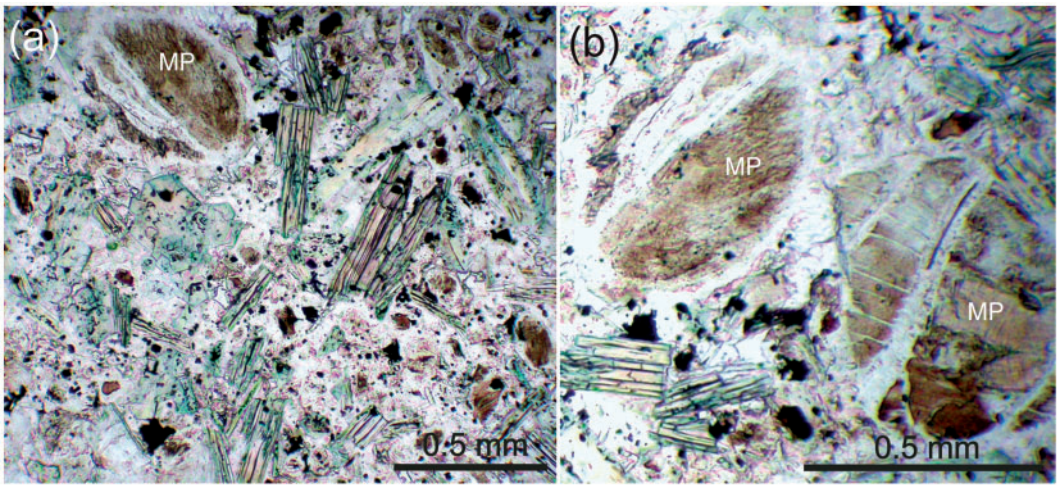

Fig. 3. Microphotographs illustrating brownish multiphase phyllosilicates (MP) (phlogopite + serpentine + talc) replacing serpentine pseudomorphs after olivine in HK4. (a) The groundmass appears as a mass of serpentine, with phlogopite pseudomorphed by chlorite, with rare relics of the original texture. (b) Multiphase phyllosilicates with multiple cleavage fractures replace serpentine pseudomorphs after two large olivine macrocrysts. Note cleavage of the phyllosilicate partially replacing serpentine. The initial round shape of the olivines is still recognizable, although cut by colourless serpentine in fractures.

olivine and the specimen's occurrence in the center of the dyke. The high olivine abundance in fig. 1c of the Gernon *et al.* Comment is evident if the field of view in photograph (c) is aligned in scale to match other photographs in the figure. The sample origin in the center of the dyke is implied by the presence of cooling joints filled with dolomite, which are present exclusively in the dyke center. All the above examples have one thing in common, the misclassification of ORK as OPK. Gernon *et al.* (2019) cannot illustrate a fresh OPK because fresh OPK, as defined by the authors, does not exist. In our opinion, the Field *et al.* (2009) Snap Lake rock classification cannot account for the mineralogical complexity of the rocks, is not internally consistent, and results in misclassification.

MINERAL COMPOSITIONS AND MAGMA BATCHES

Gernon *et al.* (2019) present compositions of phlogopites to argue for two magma batches in the Snap Lake dyke. Phlogopite is the most complex and heterogeneous mineral in these rocks (and in kimberlites in general), both compositionally and texturally. All research groups that studied Snap Lake noticed at least three different textures of phlogopite in the kimberlite. These include macrocrystal, large poikilitic, and small tabular of Kopylova *et al.* (2010), Types A–D of Ogilvie-Harris (2012), and macrocrystal, poikilitic, and tabular of Fulop *et al.* (2018), with additional division into poikilitic or non-poikilitic rims, and tabular crystals replacing serpentine as part of the multiphase phyllosilicate (Fig. 3) or granite. Phlogopites with different textures show different compositions and zoning (Kopylova *et al.*, 2010; Fulop *et al.*, 2018).

The analyses plotted by Gernon *et al.* (2019) were taken from the PhD thesis of Ogilvie-Harris (2012) and have never been reported in a peer-reviewed publication. These analyses were carried out on the same 15 thin sections as used for petrographic and SEM work (table 1 of Field *et al.*, 2009). Although Ogilvie-Harris (2012) discriminated the phlogopites based on texture, Gernon *et al.* (2019) disregard the texture and group all textural types of phlogopite in a rock type together (figs 5 and 6 of Gernon *et al.*, 2019). Furthermore, the textural context of complex phlogopite is impossible to glean in the absence of thin-section photographs, or a backscattered electron image to document the location of each phlogopite analysis in the Comment of Gernon *et al.* (2019).

In contrast, Fulop *et al.* (2018) reported (table 4 and supplementary data table S1) analyses of phlogopite and other sheet silicates from 60 thin sections of samples collected over the entire mined dyke. Each analysis location is illustrated in SEM and optical photographs showing the crystal morphology, zoning, proximity to xenoliths, and possible presence of secondary alteration. Suspicious, low-total analyses were further explored by powder and single-crystal X-ray diffractometry (XRD) on the material drilled out of thin sections.

The complexity of phlogopite chemistry is particularly acute in the Snap Lake rocks, owing to the prominent deficiency of interlayer cations; that is, (K + Ba + Na) a.p.f.u. <1. This deficiency leads to the deviation from the K–Ba inverse correlation lines for 30% (Ogilvie-Harris, 2012) to 60% of the analyses (fig. 10a, Fulop *et al.*, 2018). These analyses also plot off the global Ba + ^{IV}Al vs (KNa) + ^{IV}Si trend for kinoshitalite–phlogopite mica (fig. 12 of Tischendorf *et al.*, 2007). Ogilvie-Harris (2012) ascribed the deficiency of interlayer cations in Snap Lake phlogopites to a solid-solution with talc, despite the fact that phlogopite–talc solid-solutions with

significant deficiencies of interlayer cations have not otherwise been reported in kimberlites (Reguir *et al.*, 2009; and Fig. 4) and despite the proof that such interlayer cation-deficient phlogopites in kimberlites are multiphase intergrowths with serpentine (Sharp *et al.*, 1990), rather than a single solid-solution phase. Because the fine 50 nm sized serpentine lamellae responsible for the deficiency of 0·2–0·3 K (a.p.f.u.) (Sharp *et al.*, 1990) in phlogopite are below optical and SEM resolution, K- and Ba-deficient phlogopites cannot be presumed to be a one-phase solid-solution without TEM or XRD studies (e.g. Sharp *et al.*, 1990; Comodi *et al.*, 2011; Fulop *et al.*, 2018).

The conspicuous separation of the ORK and OPK phlogopite in fig. 5 of Gernon *et al.* (2019) has been used as the rationale for the two magma batches model. We submit that the separation results from the following shortcomings of the research methodology of Gernon *et al.* (2019).

1. The lumping of multiphase sheet silicates with phlogopites in the variation diagrams of figs 5 and 6a of Gernon *et al.* (2019), even though fig. 6b of Gernon *et al.* (2019) testifies to the significant amount of serpentine in the analyses designated as 'phlogopite'.
2. The grossly oversimplified formal tabulation of all analyses into 'cores' and 'rims'. The phlogopite growth history can only be understood on the basis of SEM images. For instance, fig. 11c of Fulop *et al.* (2018) demonstrates the highest Ba content of a grain midway between core and rim, in a complexly zoned phlogopite macrocryst with a resorbed low-Ba rim and a high-Ba poikilitic overgrowth, in which Ba decreases outward. Because Ogilvie-Harris (2012) missed the central, Ba-rich zone of phlogopite growth, her analyses yield a maximal BaO content of ~10 wt %, not capturing the high-Ba phlogopites with 13 wt % BaO, abundantly reported by Fulop *et al.* (2018), or with 18 wt % BaO reported by Kopylova *et al.* (2010).
3. The formal tabulation of all analyses into 'ORK' and 'OPK' (fig. 5 of Gernon *et al.*, 2019). By superimposing our phlogopite data, subdivided by texture, onto fig. 5 of Gernon *et al.* (2019), we demonstrate that the separation into OPK and ORK is because of the preferential occurrence of the textural varieties of phlogopite in certain rock types (Fig. 5). What Gernon *et al.* (2019) denote as OPK contains mostly

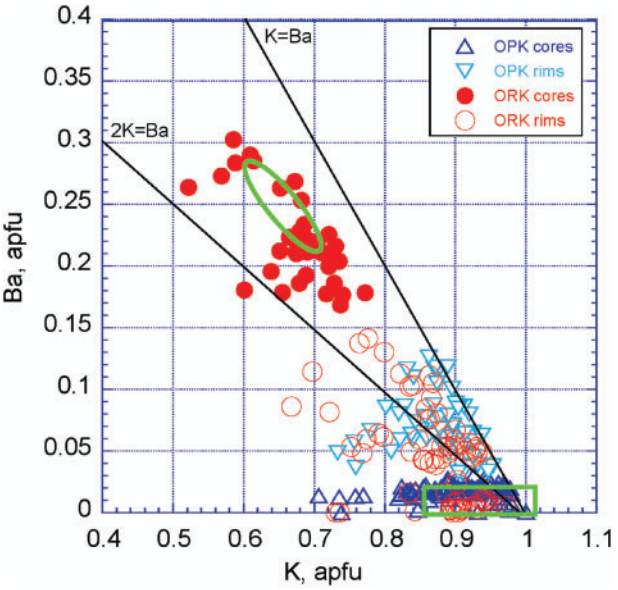

Fig. 4. The Ba vs. K (cations per formula units) plot the phlogopite reported by Ogilvie-Harris (2012). Lines with 1/2 and 1/1 Ba and K cation units observed in kimberlite phlogopite globally are from Mitchell (1986). Green open outlines are compositions of kimberlitic phlogopite macrocrysts (Reguir *et al.*, 2009) representative of the maximum deviations from the Ba-K trends.

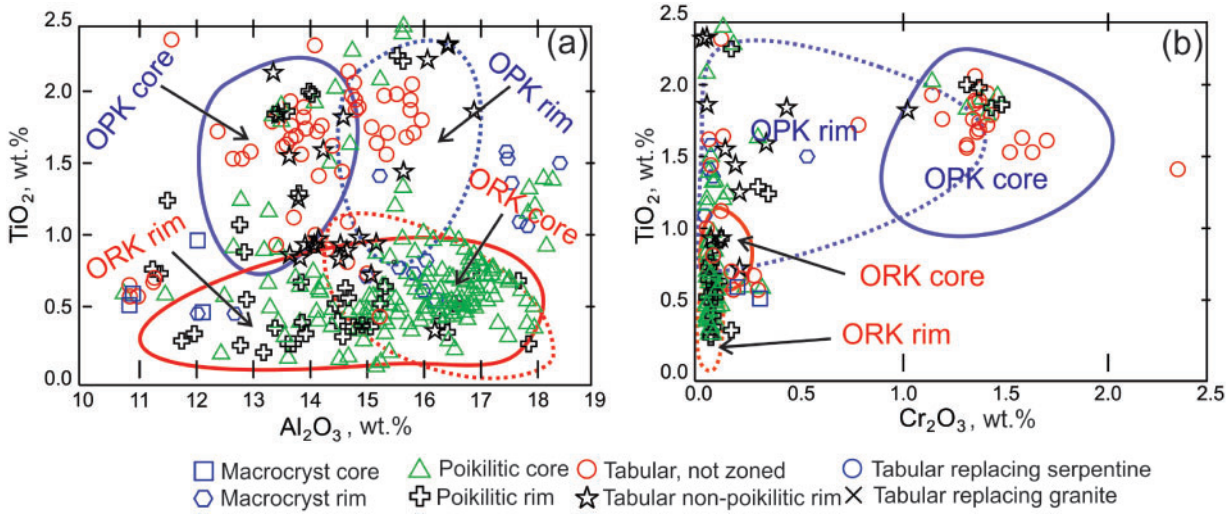

Fig. 5. Compositions of different textural types of phlogopite plotted as (a) TiO_2–Al_2O_3 (wt %) and (b) TiO_2–Cr_2O_3 (wt %). The original phlogopite data from Kopylova *et al.* (2010) are grouped according to texture as in the study by Fulop *et al.* (2018), which includes macrocrystal cores and rims, large poikilitic grains (cores and rims) and small tabular groundmass phlogopite (cores and rims). Fields for ORK cores, ORK rims, OPK cores and OPK rims are from Gernon *et al.* (2019).

tabular phlogopite, whereas ORK phlogopites are mostly poikilitic. We agree that 'cores of OPK phlogopites have lower Ba contents than cores of ORK phlogopites' (Gernon *et al.*, 2019), but an even more accurate statement should read 'tabular phlogopites have lower Ba contents than the cores of poikilitic phlogopites'. The core–rim divisions in OPK and ORK correspond to the core–rim divisions of tabular and poikilitic phlogopite. The statement 'OPK is typified by coarse-grained phlogopite phenocrysts, while ... ORK contains only fine-grained phlogopite ... of mutually exclusive unique compositions' (Field *et al.*, 2009) is not correct. Figure 4 illustrates that the OPK field contains not only tabular phlogopite, but also poikilitic; the ORK field includes not only poikilitic phlogopite, but also macrocrystal and tabular. Our observations (Fulop *et al.*, 2018) prove that all textural types of phlogopite occur in all Snap Lake rock types, and only the proportions of the phlogopite types in them vary consistently.

We conclude that the approach of Ogilvie-Harris (2012) and Gernon *et al.* (2019) cannot be a sound basis for magma batch recognition. Commonly, the assignment of kimberlite into magma batches is done with analyses of the groundmass spinel cores, as spinel is an early magmatic phase that provides the best geochemical record of the magma prior to fragmentation, crustal assimilation, and alteration processes associated with ascent and emplacement (e.g. van Straaten *et al.*, 2008; Stiefenhofer, 2013). Ogilvie-Harris (2012) wrote that 'the Cr-rich spinels are fairly similar in the two different lithofacies' (ORK and OPK), but because well-formed atoll spinel is better preserved in ORK, 'ORK underwent a much less vigorous alteration process compared to OPK'. This statement is entirely in keeping with Fulop *et al.*'s (2018) observations and petrogenetic interpretations. Even though the similar chromite chemistry and varying alteration do not disprove multiple magma batches, they better match our alternative interpretation of a single magma batch.

DIAMOND DISTRIBUTION

Contrasting diamond size frequency distributions (SFD) that support the two magma batches model (Field *et al.*, 2009) and the identical SFDs supporting the one magma batch model (Fulop *et al.*, 2018) is a crucial point in the interpretation of the Snap Lake kimberlite.

To predict the diamond grade of the kimberlite ore, two methods are most commonly used in feasibility studies of a mine prospect. The first, macrodiamond sampling, requires tonnes of ore, whereas the second, microdiamond (MIDA) sampling, requires only kilograms of kimberlite.

Field *et al.* (2009) derived two linear trends for 'hypothetical' diamond grades in OPK and ORK (fig. 8b of Field *et al.*, 2009) by bulk sampling of 17 individual samples measuring between 30 and 120 tonnes, taken from debris produced during tunnel blasting at 3 m length increments (4 m × 4 m in cross-sectional area). The volume of kimberlite taken in each sample was calculated from subsequent mapping of the tunnel walls, and the mass treated was calculated from average specific gravity measurements made from subsamples removed from the bulk sample. Each bulk sample contained varied proportions of OPK, ORK and the host granitoid (fig. 9a of Field *et al.*, 2009). In this method, the diamond grade depends on the accurate assessment of wall-rock contamination, the OPK/ORK proportions, the ore volume, and extrapolation of subsample density to the entire 3 m × 4 m × 4 m kimberlite volume. Field *et al.* (2009) admitted that 'the exact proportions of the two rock types in each bulk sample are difficult to ascertain, and the presence of ORK in OPK and *vice versa* would be unpredictable ... for hypothetical bulk sample results'. We agree that the chances of obtaining bulk samples comprising a pure lithofacies, be it rich or poor in olivine, are minimal to impossible at Snap Lake, where OPK was mapped as 20–40 cm selvages on the 3 m thick dyke (fig. 2 of Field *et al.*, 2009; fig. 4 of Gernon *et al.*, 2012). Moreover, the estimation of olivine grain size and abundance in bulk samples, either underground or on photographs, is highly inaccurate.

Microdiamond analysis was used to test the one or two magma batch models of Fulop *et al.* (2018). The drill core MIDA samples were preferred for interpretations, because of the more accurate rock classification in drill core than underground, and because crustal contamination can be better constrained with the line-scanning method. The MIDA samples included in the study by Fulop *et al.* (2018) also ensure comprehensive lateral coverage of the dyke. The microdiamond sample collection of Fulop *et al.* (2018) was based on a very strict microdiamond sampling protocol; each of 170 8 kg samples was classified based on a coinciding slab, thin section, and whole-rock chemical analysis. Only confidently classified samples (i.e. unambiguous rocks outside gradational contacts) were included in the microdiamond evaluation. In our study, the MIDA sample was labelled as HK1–HK6, as per our classification, following the petrographic and whole-rock chemical analyses. The six groups of MIDA samples were combined into two larger groups: HK1–2 in the center of the dyke corresponding to ORK, and HK3–6 at the margins of the dyke corresponding to OPK. The SFDs of the two groups overlap (fig. 17 of Fulop *et al.*, 2018), suggesting a single SFD for the entire dyke, consistent with one magma batch in the Snap Lake dyke.

Current practice in De Beers Canada and the diamond industry is to combine micro- and macrodiamond sampling for resource estimation purposes. The use of microdiamonds in combination with macrodiamonds in estimation offers advantages over the macrodiamond-only estimation, owing to increased geological confidence and reduced sampling costs. In addition, small diamonds are much more abundant than larger diamonds, considering the positively skewed (lognormal)

size distribution (Stiefenhofer *et al.*, 2016). Present and past investigations have found the microdiamond–macrodiamond relationships defined by the size frequency distribution to be continuous in individual geological units at the major De Beers mines, including Snap Lake (Stiefenhofer *et al.*, 2018). If the geological model is robust, and the units show homogeneity in the stone density or grade and a consistent SFD, the microdiamond estimation can be extrapolated to macrodiamonds (Stiefenhofer *et al.*, 2016, 2018). Further validation of the microdiamond analysis for Snap Lake is its good reconciliation against the diamond grades recovered in mining (fig. 5 of Stiefenhofer *et al.*, 2018).

We agree that the identical SFDs for HK1–2 and HK3–6 (fig. 17 of Fulop *et al.*, 2018) are not proof for the single magma batch origin of the Snap Lake kimberlite. However, the argument of Gernon *et al.* (2019) dismissing the use of diamond SFDs on account of their xenocrystal origin is inconsistent. Gernon *et al.* (2012, 2019) and Field *et al.* (2009) themselves use olivine abundances to advocate for two batches of the kimberlite magma. The xenocrystic origin of olivine in kimberlites is well known (e.g. Mitchell, 2008), and is further corroborated by the correlation between sizes and abundances of Snap Lake olivine and diamond (Field *et al.*, 2009). If diamond evidence is inadmissible, so is the olivine-related evidence for two batches of the Snap Lake magma. We, however, are not entirely certain that Gernon *et al.* (2012, 2019) accept the xenocrystal origin of olivine in kimberlite, as they refer to kimberlitic textures as 'porphyritic' and state that 'OPK magma has lost most of its phenocrystal olivines' (p. 14 of Gernon *et al.*, 2012).

ASSIMILATION AND METASOMATISM OF GRANITOID CLASTS

Gernon *et al.* (2019) question the assimilation of granite in the Snap Lake kimberlite, because of the presence of subangular, relatively fresh granite clasts in the Snap Lake dyke and the theoretical incapacity of kimberlite magma to digest granitoid clasts at shallow crustal depths.

The occasional presence of subangular, relatively fresh granite clasts does not prove the absence of granite assimilation. As we noted (Fulop *et al.*, 2018), such xenoliths occur in the Snap Lake kimberlite as an extreme end-member of the wide variety of textures showing granitoid–kimberlite interaction (figs 4, 5, 9 and fig. S6 of Fulop *et al.*, 2018). This wide spectrum of textures and morphologies of granite xenoliths is expected in the kimberlite where the timing of the xenoliths' inclusion into the melt and the corresponding intensity of the xenolith–kimberlite reaction vary (Fulop *et al.*, 2018). The choice of the photograph in fig. 6a provided by Gernon *et al.* (2019) to illustrate the granite–

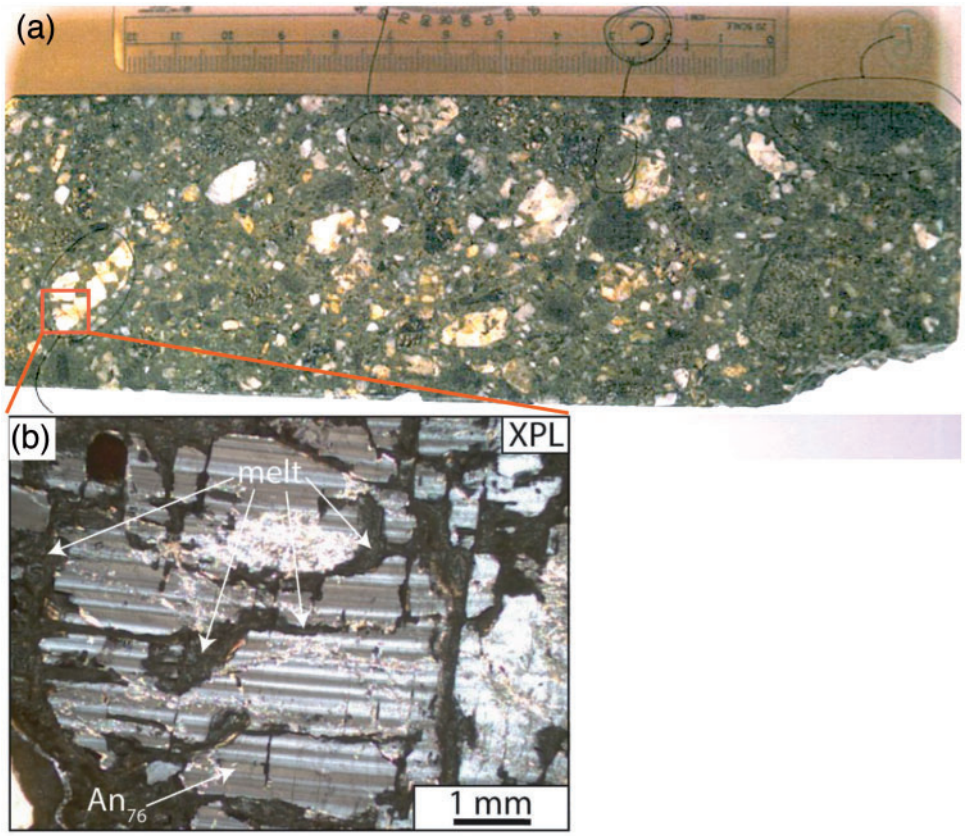

Fig. 6. (a) A general view of Renard 65 volcaniclastic kimberlite rich in granite–gneiss clasts. (b) Partial melting in one of the clasts, predominantly along cleavage planes of anorthite (An); image taken in cross-polarized light (XPL) (Gaudet *et al.*, 2018).

kimberlite relationship is troubling, because such angular, fresh xenoliths are relatively rare and are unrepresentative of the commonest appearance of granitoid xenoliths in the Snap Lake kimberlite.

The claim that 'it is not thermodynamically feasible to digest granitoid clasts in kimberlite melt at shallow crustal depths' and the arguments invoking refractory 'dry granite' in support of negligible assimilation (Gernon *et al.*, 2019) demonstrate how a theoretical dogma can supersede obvious empirical facts. Moreover, the kimberlite–granite–fluid system is neither 'dry' nor granitic in bulk composition, and the following points demonstrate the 'digestion' of granitoid clasts in kimberlite (which we divide into magmatic assimilation and subsolidus metasomatic alteration).

1. The petrographically observed sequence from pristine to partially replaced, then totally replaced and metasomatized granitoid or gneiss xenoliths in South African (Scott Smith *et al.*, 1983), Gahcho Kue (Caro *et al.*, 2004; Hetman *et al.*, 2004), Renard 65 (Gaudet *et al.*, 2018), Renard 2 (Muntener & Gaudet, 2018), and Snap Lake (Fulop *et al.*, 2018) kimberlites.
2. A documented occurrence of partially molten granitoid xenoliths in Renard 65 kimberlite (Gaudet *et al.*, 2018). There, K-feldspars exhibit molten rims with zoning from Or_{77} to Or_{95} rimward and wispy zones of melting in An_{76} crystals (Fig. 6). These features constrain temperatures to 775–900°C by comparison with phase diagrams for feldspars in wet conditions (Presnall, 1995).

The complete overprinting of the xenoliths' original textures by subsolidus metasomatic assemblages at Snap Lake does not allow for an accurate assessment of the extent and frequency of xenolith partial melting and, hence, the temperatures of the incipient assimilation. However, partial melting is not required for xenolith 'digestion' by metasomatic reactions that produce the predominant serpentine–pectolite assemblage pseudomorphing silicic clasts.

ISOCON ANALYSIS

Gernon *et al.* (2019) correctly state that classical isocon analysis (Grant, 1986; Guo *et al.*, 2009) requires designation of a pristine protolith to identify quantitative material transfers resulting from metasomatism. However, Hilchie *et al.* (2018) demonstrated that isocon analysis can be performed with respect to any reference composition, be it a primary melt, an unmodified protolith, or the least altered rock available. We are acutely aware that average HK1 is not a pristine protolith (it is altered and serpentinized), but rather is a representation of the least modified available rock unit in the Snap Lake dyke. Internal variability in HK1 is readily apparent by a cursory inspection of the diagrams (figs 15 and 18 of Fulop *et al.*, 2018; and Fig. 7 here). The diagrams that we presented in our study (Fulop *et al.*, 2018) display changes relative to the HK1 reference. A different reference would change the calculated material transfers, but the relationships between samples remain the same. Thus, comparing trend lines from unit to unit is equally valid with whatever choice of reference rock.

Gernon *et al.* (2019) also assert that the isocon modelling of Fulop *et al.* (2018) involves circular reasoning, as it implicitly regards HK6 (and other units) as having similar original compositions (i.e. deriving from the same magma batch) to that of HK1. This assertion simply misconstrues our use of the isocon method. We did not present the isocon results as evidence of either a single magma batch or derivation of HK6 by alteration and assimilation. The exhaustive field, petrographic, and mineralogical observations (Fulop *et al.*, 2018) are the evidence for metasomatism and assimilation as the causes of lithological variation at Snap Lake. The isocon modelling is a semi-quantitative portrayal of the effects of metasomatism.

HYDROUS FLUID SOURCES

The two models of Snap Lake kimberlite formation were viewed by Gernon *et al.* (2019) as diverging on the origin of water in the Snap Lake kimberlite. This

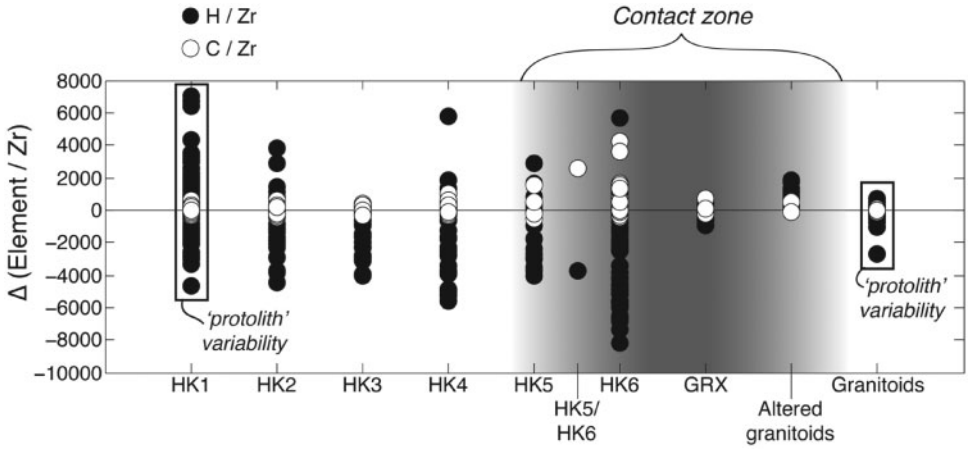

Fig. 7. Stoichiometric changes in H_2O (black) and CO_2 (white) abundance in rock compositions HK1–HK6 and in the granite near the contact. Changes are calculated from Zr-normalized rock compositions (Guo *et al.*, 2009) using the updated isocon method (Hilchie *et al.*, 2018), as well as projection procedures to account for physical mixing between the main lithologies.

perception is incorrect. Both models agree that the H_2O component of the Snap Lake bulk composition may combine deuteric and externally derived water. Gernon *et al.* (2019) admit the presence of magmatic water, but argue for groundwater as the only plausible source of predominant alteration. The limit of 2·0 wt % of deuteric water was calculated by Gernon *et al.* (2019) based on the wrong lithostatic pressure of 20 MPa for 2 km depth and 10 MPa overpressure for dyke emplacement. Fulop *et al.* (2018) constrained the origin of volatiles only for the first stage of the subsolidus alteration, which dissolved perovskite, partly serpentinized olivine and led to calcite dolomitization. Because an acidic fluid is requisite for leaching calcic minerals, a low-pH magmatic CO_2–H_2O fluid, rather than meteoric water, would be a natural choice for the fluid. We did not comment on the source of fluid for extensive serpentinization and metasomatism subsequent to the initial serpentinization of the kimberlite. The distinction between the initial serpentinization and the later advanced alteration is based on comparison of Snap Lake with other hypabyssal kimberlites. The typical serpentinization of monticellite and partial serpentinization of olivine, in our view, is a threshold between the inescapable deuteric stage of the kimberlite alteration and the later, superfluous alteration. At Snap Lake, the more intense and advanced alteration is indeterminate by source and requires additional data analysis.

The bulk composition and mineralogy of Snap Lake's HK1 is H_2O-rich and CO_2-poor in comparison with proposed primary kimberlite and other hypabyssal kimberlites. Indeed, the kimberlite bulk estimates have 5–9 wt % H_2O and 5–12 wt % CO_2 (Kopylova *et al.*, 2007; Stamm & Schmidt, 2017), which bracket observed compositions of hypabyssal kimberlites (average 7·2 wt % H_2O and 4·8 wt % CO_2; Kjarsgaard *et al.*, 2009). Snap Lake bulk-rock HK1 has ~12 wt % H_2O and only 3 wt % CO_2 (Table 1). Such compositions match the anomalously high and low modes of interstitial groundmass serpentine and groundmass carbonate, respectively, in HK1.

The bulk water content typical of minimally surficially altered and crustally contaminated hypabyssal kimberlites is up to 7 wt % H_2O (Kjarsgaard *et al.*, 2009). The origin of this water is a matter of longstanding controversy (e.g. Mitchell, 2008; Brooker *et al.*, 2011; Moussallam *et al.*, 2016). We accept that at least some of this 7 wt % H_2O is deuteric, and a minimum of ~5 wt % H_2O present in HK1 (12 wt % H_2O in HK1 less 7 wt % H_2O in the average hypabyssal kimberlite) is probably externally derived.

Gernon's comparison of the H_2O solubility in the kimberlite melt and its comparison with the alleged 25–30 wt % H_2O in the Snap Lake magma totally misses the point, as Fulop *et al.* (2018) never stated that all H_2O in the bulk Snap Lake kimberlite analysis is deuteric. We also found that the assertion of 'the penetration of the groundwater into the cooling intrusion during emplacement' (Gernon *et al.*, 2019) contradicts the overpressure of magma and deuteric water in their model. Hydrous haloes around kimberlites (Tappert & Tappert, 2018) attest to the opposite; that is, the flow of the deuteric water ~175 m into the adjacent country-rock.

The behaviour of water within the Snap Lake kimberlite system is more complex than simple enrichment over typical hypabyssal kimberlite. We extended the isocon method used by Fulop *et al.* (2018) to constrain the behaviour of volatiles in the metasomatized kimberlites in contact with granitoids. We recalculated the bulk analyses from supplementary data table S3 of Fulop *et al.* (2018) to assess the amount of H_2O and CO_2 (in wt %) in variously altered Snap Lake kimberlites (Table 1). The resulting diagram (Fig. 7) illustrates a relative depletion of H with increasing contamination and metasomatism, and the opposite trend for C. The isocon results confirm the mineralogical and bulk compositional properties of the rocks. HK1 is already very water-rich owing to the abundant serpentine, which completely pseudomorphs olivine and monticellite (>65% vol. %). The bulk compositions of the metasomatized rocks HK3–6 are less water-rich than those of the less metasomatized ones (Table 1) and consistent with the lower atomic abundance of H in the HK3–6 assemblage. As the granite-related metasomatism replaces serpentine with phlogopite and talc in HK3–HK6, a net loss of water from the rock is expected. Indeed, serpentine has a greater proportion of H than talc or phlogopite—ideal Mg-serpentine is ~22 atomic % H, phlogopite is only ~8% and talc is ~9%. The phyllosilicate alteration assemblage of serpentine + phlogopite + talc can form by a loss of water from a serpentine-rich HK1 'protolith'. Part of this trend may be related to H_2O dilution because of the higher abundance of granite xenoliths in HK3–6 rocks (Table 1).

Table 1: Fluid components of the Snap Lake bulk composition

Sample	HK1	HK2	HK3	HK4	HK5	HK6	Carbonatized HK6
Rock type	Av. of 93	Av. of 30	Av. of 19	Av. of 23	Av. of 12	Av. of 42	Av. of 5
LOI (wt %)	15·5	14·7	14·8	14·6	14·1	13·6	22·0
CO_2 (wt %)	2·6	2·5	3·2	3·3	2·9	3·5	13·5
H_2O (wt %)	12·9	12·3	11·6	11·3	11·2	10·0	8·5
Δ(H/Zr) (atomic)	263·8	–979·0	–2166·2	–2183·8	–1260·6	–3489·7	–3·046·1
Abundance of granite xenoliths >1 cm (vol. %)	<5	1–15	5–10	10	10–15	10–15	

LOI, loss on ignition. CO_2 is calculated based on measured total C under assumption of negligible carbon outside carbonate. H_2O is calculated as LOI-CO_2.

Petrographic observations at Snap Lake demonstrate the extreme ease of recrystallization and overprinting of primary kimberlite mineralogy, and partly explain the meteoric origin of their stable isotopic signatures (Mitchell, 2013; Giuliani *et al.*, 2014).

CONCLUSIONS

The Snap Lake kimberlite debate emphasizes the pivotal role of methodology in correct interpretation of magmatic bodies; that is, the good familiarity with the rocks necessary for selection of representative samples, sampling that covers all dimensions of the magmatic body, and textural observations in thin sections guiding further analytical techniques.

Omissions to this method may lead to incorrect conclusions regarding even the simplest magmatic body, a dyke, and would be even more detrimental for complex multi-phase bodies. For kimberlite research, such sound methodology requires close collaboration with the owner company and mine or exploration geologists for data collection over a long period of time.

REFERENCES

Brooker, R. A., Sparks, R. S. J., Kavanagh, J. L. & Field, M. (2011). The volatile content of hypabyssal kimberlite magmas: some constraints from experiments on natural rock compositions. *Bulletin of Volcanology* **73**, 959–981.

Caro, G., Kopylova, M. G. & Creaser, R. A. (2004). The hypabyssal 5034 kimberlite of the Gahcho Kue cluster, Southeastern Slave Craton, Northwest Territories, Canada: a granite-contaminated Group-I kimberlite. *Canadian Mineralogist* **42**, 183–207.

Comodi, P., Nazzareni, S., Fumagalli, P. & Capitani, G. C. (2011). The peculiar crystal-chemistry of phlogopite from metasomatized peridotites: evidence from laboratory and nature. *Periodico di Mineralogia* **80**, 181–197.

Field, M., Gernon, T. M., Mock, A., Walters, A., Sparks, R. S. J. & Jerram, D. A. (2009). Variations of olivine abundance and grain size in the Snap Lake kimberlite intrusion, Northwest Territories, Canada: a possible proxy for diamonds. *Lithos* **112S**, 23–35.

Fulop, A., Kopylova, M., Kurszlaukis, S., Hilchie, L., Ellemers, P. & Squibb, C. (2018). Petrography of Snap Lake kimberlite dyke (Northwest Territories, Canada) and its interaction with country rock granitoids. *Journal of Petrology* **59**, 2493–2518.

Gaudet, M., Kopylova, M., Muntener, C., Zhuk, V. & Nathwani, C. (2018). Geology of the Renard 65 kimberlite pipe, Québec, Canada. *Mineralogy and Petrology* **112**(Supplement 2), 433–445.

Gernon, T. M., Field, M. & Sparks, R. S. J. (2012). Geology of the Snap Lake kimberlite intrusion, Northwest Territories, Canada: field observations and their interpretation. *Journal of the Geological Society, London* **169**, 1–16.

Gernon, T., Sparks, R. S., Field, M., Ogilvie-Harris, R., Schumacher, J. & Brooker, R. (2019). Comment on: 'Petrography of Snap Lake kimberlite dyke (Northwest Territories, Canada) and its interaction with country rock granitoids'. *Journal of Petrology* **60**, 000–000.

Giuliani, A., Phillips, D., Kamenetsky, V. S., Fiorentini, M. L., Farquhar, J. & Kendrick, M. A. (2014). Stable isotope (C, O, S) compositions of volatile-rich minerals in kimberlites: a review. *Chemical Geology* **374–375**, 61–83.

Grant, J. A. (1986). The isocon diagram; a simple solution to Gresens' equation for metasomatic alteration. *Economic Geology* **81**, 1976–1982.

Guo, S., Ye, K., Chen, Y. & Liu, J. B. (2009). A normalization solution to mass transfer illustration of multiple progressively altered samples using the isocon diagram. *Economic Geology* **104**, 881–886.

Hetman, C. M., Scott Smith, B. H., Paul, J. L. & Winter, F. W. (2004). Geology of the Gahcho Kue kimberlite pipes, NWT, Canada: root to diatreme transition zones. *Lithos* **76**, 51–74.

Hilchie, L., Russell, J. K. & Stanley, C. (2018). Unification of isocon and Pearce element ratio techniques in the quantification of material transfer. *Economic Geology* **113**, 1608–1618.

Kjarsgaard, B. A., Pearson, D. G., Tappe, S., Nowell, G. M. & Dowall, D. P. (2009). Geochemistry of hypabyssal kimberlites from Lac de Gras, Canada: comparisons to a global database and applications to the parent magma problem. *Lithos* **112S**, 236–248.

Kopylova, M. G., Matveev, S. & Raudsepp, M. (2007). Searching for parental kimberlite melt. *Geochimica et Cosmochimica Acta* **71**, 3616–3629.

Kopylova, M. G., Mogg, T. & Scott Smith, B. (2010). Mineralogy of the Snap Lake kimberlite, Northwest Territories, Canada, and compositions of phlogopite as records of its crystallization. *Canadian Mineralogist* **48**, 549.

Mitchell, R. H. (1986). *Kimberlites: Mineralogy, Geochemistry and Petrology*. New York: Plenum.

Mitchell, R. H. (2008). Petrology of hypabyssal kimberlites: relevance to primary magma compositions. *Journal of Volcanology and Geothermal Research* **174**, 1–8.

Mitchell, R. H. (2013). Oxygen isotope studies of serpentine in kimberlite. In: Pearson, D. G., Grutter, H. S., Harris, J. W., Kjarsgaard, B. A., O'Brien, H., Rao, N. V. C. & Sparks, S. (eds.) *Proceedings of the 10th International Kimberlite Conference*, Vol. 1, Springer, New Delhi, pp. 1–12.

Moussallam, Y., Morizet, Y. & Gaillard, F. (2016). H_2O–CO_2 solubility in low SiO_2-melts and the unique mode of kimberlite degassing and emplacement. *Earth and Planetary Science Letters* **447**, 151–160.

Muntener, C. & Gaudet, M. (2018). Geology of the Renard 2 pipe to 1000-m depth, Renard Mine, Québec, Canada: insights into Kimberley-type pyroclastic kimberlite emplacement. *Mineralogy and Petrology* **112**(Supplement 2), 421–432.

Ogilvie-Harris, R. C. (2012). Constraining the nature of kimberlite melts by textural, compositional and experimental methods. PhD thesis, Bristol University.

Presnall, D. C. (1995). Phase diagrams of earth-forming minerals. In: Ahrens, T. J. (ed.) *Mineral Physics and Crystallography: A Handbook of Physical Constants*. Washington, DC: American Geophysical Union, pp. 246–268.

Reguir, E. P., Chakhmouradian, A. R., Halden, N. M., Malkovets, V. G. & Yang, P. (2009). Major- and trace-element compositional variation of phlogopite from kimberlites and carbonatites as a petrogenetic indicator. *Lithos* **112S**, 372–384.

Scott Smith, B. H., Skinner, E. M. W. & Clement, C. R. (1983). Further data on the occurrence of pectolite in kimberlite. *Mineralogical Magazine* **47**, 75–78.

Sharp, T., Otten, M. T. & Buseck, P. R. (1990). Serpentinization of phlogopite phenocrysts from a micaceous kimberlite. *Contributions to Mineralogy and Petrology* **104**, 530–539.

Stiefenhofer, J. (2013). The use of chemical and metallurgical parameters to enhance the economic value of kimberlite resource models. In: *Proceedings of the 5th Conference Diamonds—Source to Use*. Johannesburg: Southern African Institute of Mining and Metallurgy, pp. 73–84.

Stiefenhofer, J., Thurston, M. L., Rose, D. M., Chinn, I. L. & Ferreira, J. J. (2016). Principles of using microdiamonds for resource estimation: 1—The impact of mantle and kimberlite processes. *Canadian Institute of Mining, Metallurgy and Petroleum* **7**, 216–238.

Stiefenhofer, J., Thurston, M. L. & Bush, D. E. (2018). Microdiamond grade as a regionalised variable—some basic requirements for successful local microdiamond resource estimation of kimberlites. *Mineralogy and Petrology* **112**(Supplement 2), 673–684.

Stamm, N. & Schmidt, N. W. (2017). Asthenospheric kimberlites: volatile contents and bulk compositions at 7-GPa. *Earth and Planetary Science Letters* **474**, 309–321.

Tappert, M. C. & Tappert, R. (2018). *Novel exploration tools: using reflectance spectroscopy to detect hydration halos around kimberlites. Northwest Territories Geological Survey, NWT Open Report* 2018-012, 39 pp.

Tischendorf, G., Forster, H.-J., Gottesmann, B. & Rieder, M. (2007). True and brittle micas: composition and solid-solution series. *Mineralogical Magazine* **71**, 285–320.

van Straaten, B., Kopylova, M., Russell, J., Webb, K. & Scott Smith, B. H. (2008). Discrimination of diamond resource and non-resource domains in the Victor North pyroclastic kimberlite, Canada. *Journal of Volcanology and Geothermal Resource* **174**, 128–138.